

Glycodendrimersomes from Sequence-Defined Janus Glycodendrimers Reveal High Activity and Sensor Capacity for the Agglutination by Natural Variants of Human Lectins

Shaodong Zhang,[†] Qi Xiao,[†] Samuel E. Sherman,[†] Adam Muncan,[†] Andrea D. M. Ramos Vicente,[†] Zhichun Wang,[‡] Daniel A. Hammer,[‡] Dewight Williams,[§] Yingchao Chen,^{||} Darrin J. Pochan,^{||} Sabine Vértesy,[⊥] Sabine André,[⊥] Michael L. Klein,[#] Hans-Joachim Gabius,[⊥] and Virgil Percec^{*,†}

[†]Roy & Diana Vagelos Laboratories, Department of Chemistry, University of Pennsylvania, Philadelphia, Pennsylvania 19104-6323, United States

[‡]Department of Chemical and Biomolecular Engineering, University of Pennsylvania, Philadelphia, Pennsylvania 19104-6391, United States

[§]Electron Microscopy Resource Laboratory, Perelman School of Medicine, University of Pennsylvania, Philadelphia, Pennsylvania 19104-6082, United States

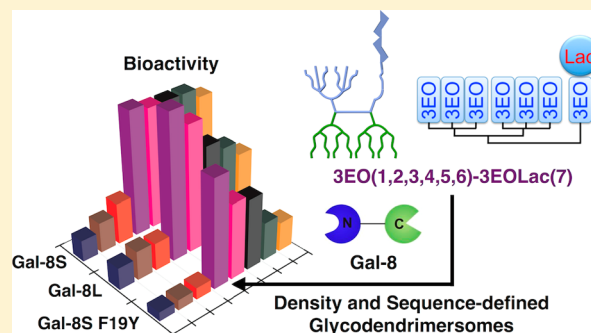
^{||}Department of Materials Science & Engineering, University of Delaware, Newark, Delaware 19716, United States

[⊥]Institute of Physiological Chemistry, Faculty of Veterinary Medicine, Ludwig-Maximilians-University, Veterinärstrasse 13, 80539 Munich, Germany

[#]Institute of Computational Molecular Science, Temple University, Philadelphia, Pennsylvania 19122, United States

S Supporting Information

ABSTRACT: A library of eight amphiphilic Janus glycodendrimers (Janus-GDs) presenting D-lactose (Lac) and a combination of Lac with up to eight methoxytriethoxy (3EO) units in a sequence-defined arrangement was synthesized via an iterative modular methodology. The length of the linker between Lac and the hydrophobic part of the Janus-GDs was also varied. Self-assembly by injection from THF solution into phosphate-buffered saline led to unilamellar, monodisperse glycodendrimersomes (GDSs) with dimensions predicted by Janus-GD concentration. These GDSs provided a toolbox to measure bioactivity profiles in agglutination assays with sugar-binding proteins (lectins). Three naturally occurring forms of the human adhesion/growth-regulatory lectin galectin-8, Gal-8S and Gal-8L, which differ by the length of linker connecting their two active domains, and a single amino acid mutant (F19Y), were used as probes to study activity and sensor capacity. Unpredictably, the sequence of Lac on the Janus-GDs was demonstrated to determine bioactivity, with the highest level revealed for a Janus-GD with six 3EO groups and one Lac. A further increase in Lac density was invariably accompanied by a substantial decrease in agglutination, whereas a decrease in Lac density resulted in similar or lower bioactivity and sensor capacity. Both changes in topology of Lac presentation of the GDSs and seemingly subtle alterations in protein structure resulted in different levels of bioactivity, demonstrating the presence of regulation on both GDS surface and lectin. These results illustrate the applicability of Janus-GDs to dissect structure–activity relationships between programmable cell surface models and human lectins in a highly sensitive and physiologically relevant manner.



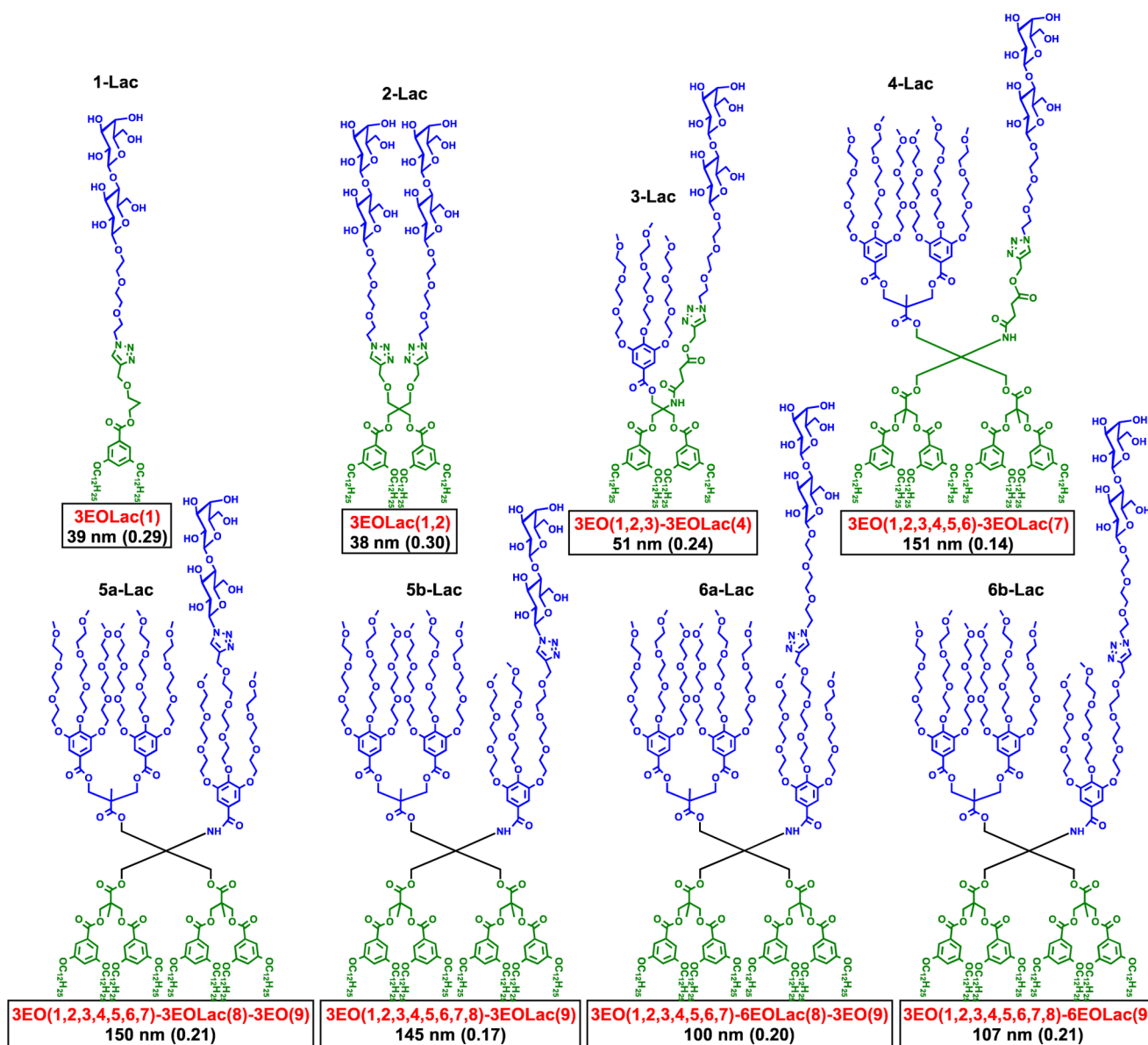
INTRODUCTION

One of the key challenges of current biomedical research is to gain an understanding of the molecular basis of cell–cell/matrix interactions. It is known that already at the stage of sperm–zona pellucida recognition in fertilization, various binding parameters, such as the epitope structure of determinants and their local density and topology of presentation, cooperate to generate the required avidity, selectivity, specificity, and contact stability of binding.¹ Increasingly gaining attention, loading and delivery of exosomes and microvesicles, with diameters from 40 to about

150 nm or more, are likewise of central biological relevance as a means for directed transport and understanding mechanisms of assembly.² Prominent among surface interactions is the interplay between glycans and their receptors (lectins), which is involved in many physiological and pathological processes.³ However, although the nominal carbohydrate specificity of lectins is being characterized in detail, the intriguing selectivity of this

Received: August 20, 2015

Published: September 30, 2015

Scheme 1. Summary of Amphiphilic Janus Dendrimers with Different Density and Sequence-Defined Arrangement of D-Lactose (Lac) in the Hydrophilic Segment^a

^aCodes of the amphiphilic molecules are indicated in black and their short notations are indicated in red. The diameter (D_{DLS} , in nm) and polydispersity (in parentheses) were determined by dynamic light scattering (DLS) at 0.1 mM of Lac in phosphate-buffered saline (PBS 1×).

recognition mode on cell and vesicle surfaces indicates that topological factors can play major roles. To address this issue, the design and synthesis of readily programmable model systems is a challenge for supramolecular chemistry. Access to these models will enable an understanding of the contributions of structure, topology of presentation, and particle size on bioactivity toward human lectins.

So far, two different strategies have been employed to prepare tools for unraveling the complexity of carbohydrate–lectin interactions, including a covalent approach with synthetic glycopeptides,⁴ glycopolymers,⁵ and glycodendrimers⁶ and a supramolecular approach⁷ including glycan-presenting vesicles. For example, the Kiessling laboratory observed in a model study that a higher density of carbohydrates on glycopolymers^{5d} results in increased activity per polymer but decreased efficiency per carbohydrate toward lectins, while the Kick laboratory found

increased relative activity to carbohydrate ligands at lower density of binding epitopes on a glycopolymer.^{5e} The Seeberger laboratory designed programmable sequences of carbohydrates on monodisperse glycooligomers and concluded that the increase of the number of sugars from one to three enhanced the relative activity,⁵ⁱ while dilution with noncognate sugars on these glycooligomers improved the relative activity.⁵ⁿ Although these pioneering approaches provided valuable insight into the “multivalency” of glycan ligands,^{3b,8} they also demonstrated that the influence of ligand structure on the mechanism of carbohydrate–lectin interaction process is incompletely understood.^{5d,e,i,n,l,7a} For example, the previous mimics of biological membranes could not closely model their surface with spatial display of glycan ligands containing an optimal density and defined sequence. With the aim to design such biological mimics, glycodendrimersomes (GDSs),⁹ which provide access to density

and sequence control, were recently introduced. They are generated by the self-assembly of amphiphilic Janus-glycodendrimers (Janus-GDs) and have potent bioactivity as docking sites for lectins, establishing a model system for studying their trans-bridging capacity.^{9b-d} In this study, eight sequence- and density-defined Janus-GDs were synthesized and shown to self-assemble into unilamellar GDSs of predictable dimensions. Agglutination assays of the GDSs were performed with the biomedically relevant human lectin galectin-8 to reveal an optimal glycan topology that unexpectedly occurs for a low density of D-lactose (Lac) in a defined sequence to generate the highest agglutination relative activity and sensor capacity.

RESULTS AND DISCUSSION

Rational Design and Iterative Modular Synthesis of Amphiphilic Janus Dendrimers with Density- and Sequence-Defined D-Lactose. A distinctive feature of the presence of glycans on the cell surface is the natural heterogeneity of density. It can be based on microclusters such as branching of N-glycans and mucin-type O-glycans. It can also be based on macroclusters referring to the local vicinity of individual glycan chains in glycoproteins, such as mucins, or in microdomains with glycoprotein/glycolipid clusters. It was previously reported that bioinspired GDSs self-assembled from “single–single” (1-Lac), “twin–twin” (2-Lac), and “twin–mixed” (3-Lac) amphiphilic Janus-GDs (Scheme 1) and their D-mannose (Man)-containing analogues.^{9b} With agglutination assays of GDSs with identical concentration of carbohydrates, it was discovered that GDSs self-assembled from 3-Lac or its Man-containing analogue with a lower density of glycan ligands exhibited higher relative bioactivity toward their cognitive lectins.^{9b-d} However, no optimal density and sequence of carbohydrate toward glycan ligands on biological membranes was determined. This fundamental question prompted the design of new Janus-GDs from 4-Lac to 6-Lac (Scheme 1) with increasingly reduced density and defined sequences of epitopes. The general aim was to gain fundamental insight into the multivalency and the impact of topology of glycan presentation and also to attempt to find out if an optimal density and sequence of glycan ligands providing the highest activity can be realized.

Inspired by the notation coined by the Seeberger laboratory,^{5m} the amphiphilic molecules designed for the current study are denoted with the self-explanatory notations illustrated in Figure 1. Taking 3EO(1,2,3)-3EOLac(4) for example, “3EO” denotes the methoxytriethoxy group, “3EOLac” refers to the triethoxylactoside group, and the numbers within the parentheses define the position of each hydrophilic tail in the hydrophilic segment. These molecules were also given a code such as 3-Lac. Together with Scheme 1, Figure 1 demonstrates the rational design of the series of Lac-containing Janus-GDs. As described previously by our laboratory,^{9b} 1-Lac [3EOLac(1)] contains a single hydrophobic first-generation minidendron and a single carbohydrate headgroup, which simply reduces its molecular weight by half compared to 2-Lac [3EOLac(1,2)]. Of note, these two molecular frameworks share the same density of Lac. Comparing to 1-Lac and 2-Lac, the density of Lac in 3-Lac [3EO(1,2,3)-3EOLac(4)] is reduced by introducing three chains of 3EO in the hydrophilic part. From 3-Lac to 4-Lac [3EO(1,2,3,4,5,6)-3EOLac(7)] and to 5a-Lac [3EO(1,2,3,4,5,6,7)-3EOLac(8)-3EO(9)] and to 5b-Lac [3EO(1,2,3,4,5,6,7,8)-3EOLac(9)], the density of Lac further decreases. 5a-Lac and 5b-Lac [3EO(1,2,3,4,5,6,7,8)-3EOLac(9)] are a pair of isomers with Lac located in different positions on the hydrophilic segment, and the same is true for 6a-Lac [3EO(1,2,3,4,5,6,7)-6EOLac(8)-3EO(9)] and 6b-Lac [3EO(1,2,3,4,5,6,7,8)-6EOLac(9)].

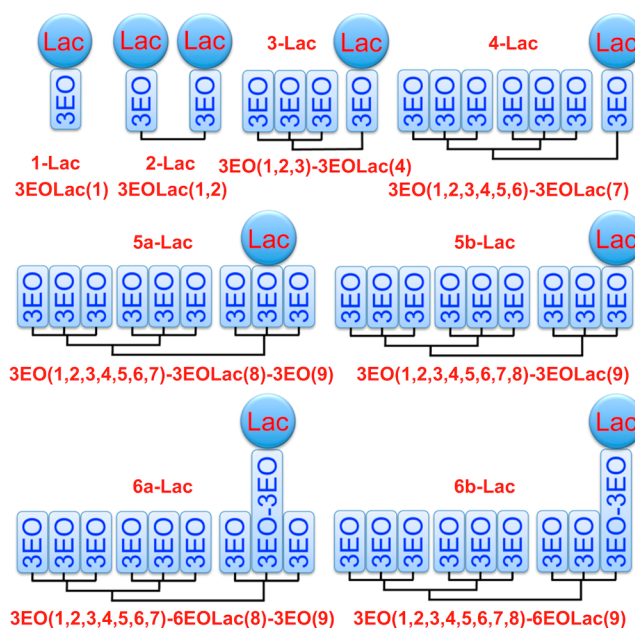


Figure 1. Summary of Lac-containing amphiphilic Janus dendrimers used for agglutination assays with galectin-8 (3EO = methoxytriethoxy group and Lac = D-lactose). The hydrophobic segments of these molecules, triazoles, and aromatic rings are omitted for clarity. The numbers in the parentheses define the position of each hydrophilic tail that is counted from the left to the right of each molecule.

3EO(9)] and 6b-Lac [3EO(1,2,3,4,5,6,7,8)-6EOLac(9)]. Compared to 5a-Lac/5b-Lac, 6a-Lac/6b-Lac are only different in that their Lac headgroups are attached to a longer chain of oligo(ethylene glycol) monomethyl ether.

In accordance with the method used for the synthesis of the “twin–mixed” molecule 3-Lac previously reported,^{9b} 4-, 5a-, 5b-, 6a- and 6b-Lac were synthesized via an accelerated modular strategy by using acetone-protected tris(hydroxymethyl)aminomethane (Tris) (5) to form the Janus dendrimers with three different groups (A, B, C), as outlined in Figure 2. First, the presence of the amino group in 5, which allowed for the selective addition of an acid- or anhydride-containing group A to the amino group in molecule 5, was realized via amidation. The presence of a single unprotected hydroxyl group on the resulting molecules (6, 20a, 20b) allowed for the targeted addition of an acid containing the hydrophilic group B. This esterification yielded the desired hydrophilic portion of the Janus dendrimers (7, 21a, 21b). Their acetone groups were then removed via acid catalysis to yield two hydroxyl groups in the resulting products (8, 22a, 22b). Esterification of the hydroxyl groups in 8, 22a, and 22b with an acid-containing group C was performed to generate the hydrophobic portion of the Janus dendrimers. Finally, the modular synthesis was completed with the addition of two possible azide-functionalized D-lactose derivatives (Lac-3EO-N₃ or Lac-N₃) to the alkyne in group A of the hydrophilic portion of the Janus dendrimers via copper-catalyzed click chemistry¹⁰ to give 4-, 5a-, 5b-, 6a-, and 6b-Lac. Detailed reagents and conditions for each reaction are presented in Schemes S1–7 (Supporting Information, SI).

Self-Assembly of Lac-Containing Janus-GDs into Monodisperse, Unilamellar GDSs with Predictable Size. The GDSs were prepared by injection of their THF solution into PBS.^{9,11} As determined by cryogenic transmission electron microscopy (cryo-TEM), all Lac-containing Janus-GDs self-

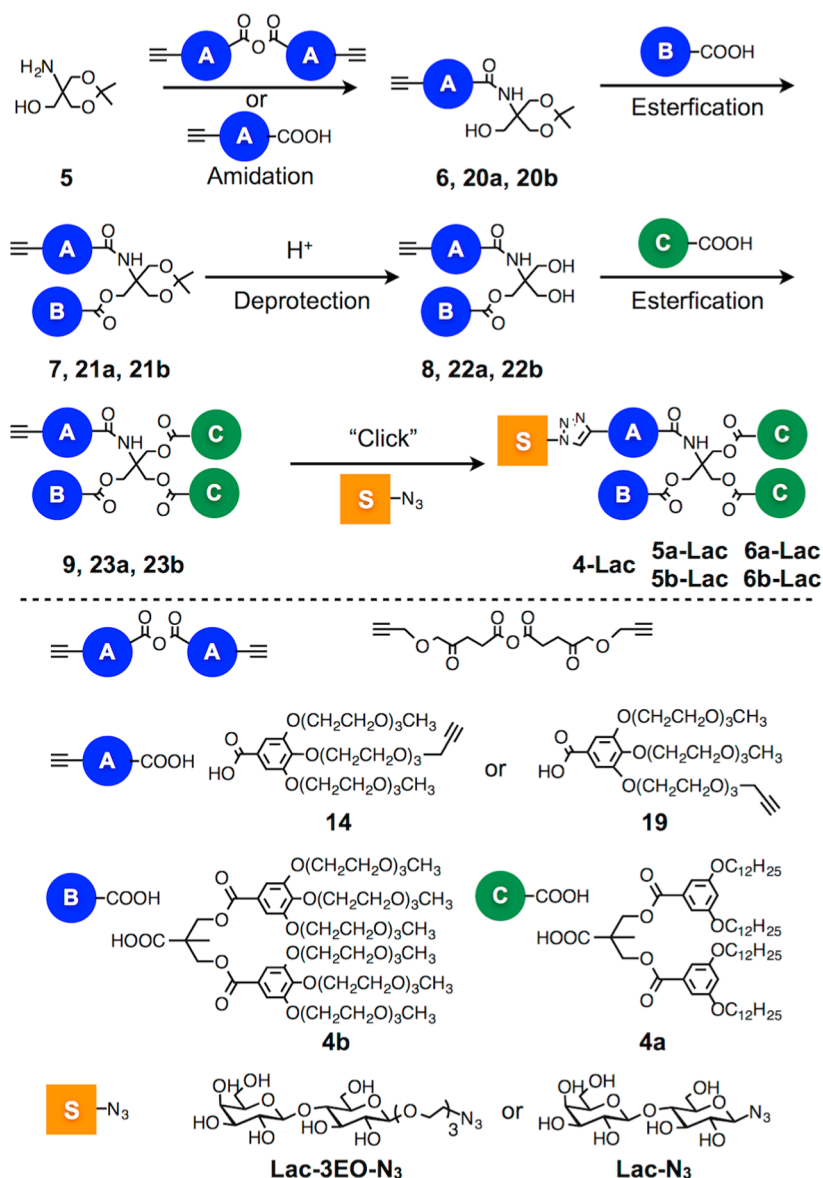


Figure 2. Summary of the accelerated iterative modular synthetic strategy employed in the preparation of the amphiphilic Janus-GDs **4-Lac**, **5a-Lac**, **5b-Lac**, **6a-Lac**, and **6b-Lac**. “A” represents the structure incorporated in the dendrimers between the triazole ring and the Tris framework, “B” represents a second-generation hydrophilic minidendron, “C” represents a second-generation hydrophobic minidendron, and “S” represents the Lac group.

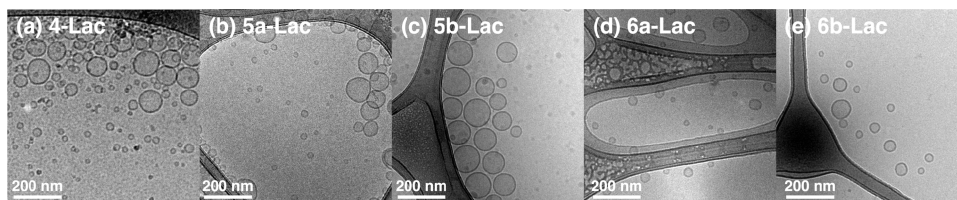


Figure 3. Selected cryo-TEM images of GDSs self-assembled by amphiphilic molecules (a) **4-Lac** [3EO(1,2,3,4,5,6)-3EOlac(7)], (b) **5a-Lac** [3EO(1,2,3,4,5,6,7)-3EOlac(8)-3EO(9)], (c) **5b-Lac** [3EO(1,2,3,4,5,6,7,8)-3EOlac(9)], (d) **6a-Lac** [3EO(1,2,3,4,5,6,7)-6EOlac(8)-3EO(9)], and (e) **6b-Lac** [3EO(1,2,3,4,5,6,7,8)-6EOlac(9)] at 0.1 mM in PBS.

assemble into unilamellar vesicles in PBS. Representative images of **4-**, **5a-**, **5b-**, **6a-**, and **6b-Lac** GDSs are shown in **Figure 3**. Images of **1-**, **2-**, and **3-Lac** have been reported previously.^{9b}

Dynamic light scattering (DLS) was used to assess differences in diameter of GDSs prepared with the same molar concentration of Lac (0.1 mM) in PBS. As shown in **Scheme 1** and **Figure 4**, the size and size-distribution of the vesicles self-

assembled from **1-Lac** and **2-Lac** are almost identical. Considering that **1-Lac** shares similar chemical structure with half of **2-Lac**, this identical self-assembly behavior (**Figure 4**) indicates that the power of two molecules of **1-Lac** is equal to that of one molecule of **2-Lac** during the self-assembly process. Intuitively, the volume occupied by an individual molecule in a GDS should increase with the molecular weight of the Janus-GD,

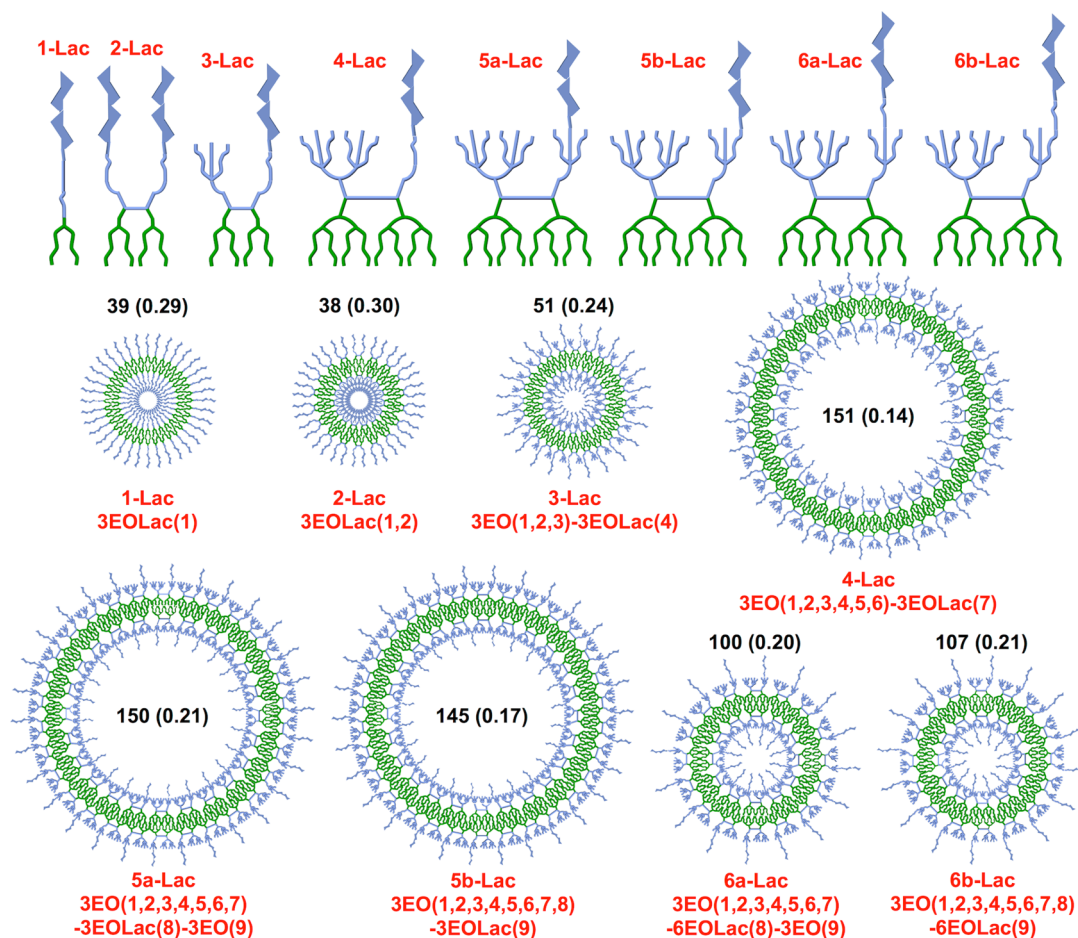


Figure 4. Short notations and the summary of Lac-containing amphiphilic molecules with different topologies and their corresponding GDSs. The diameter (D_{DLS} , in nm) and polydispersity (in the parentheses) were measured by DLS (0.1 mM of Lac in PBS). 3D topological vesicular structures are drawn as 2D cross-sectional models for better clarify of their surface arrangement and density of glycans. For simplicity, Lac groups are isolated, although most probably they interact with each other during the self-assembly process.

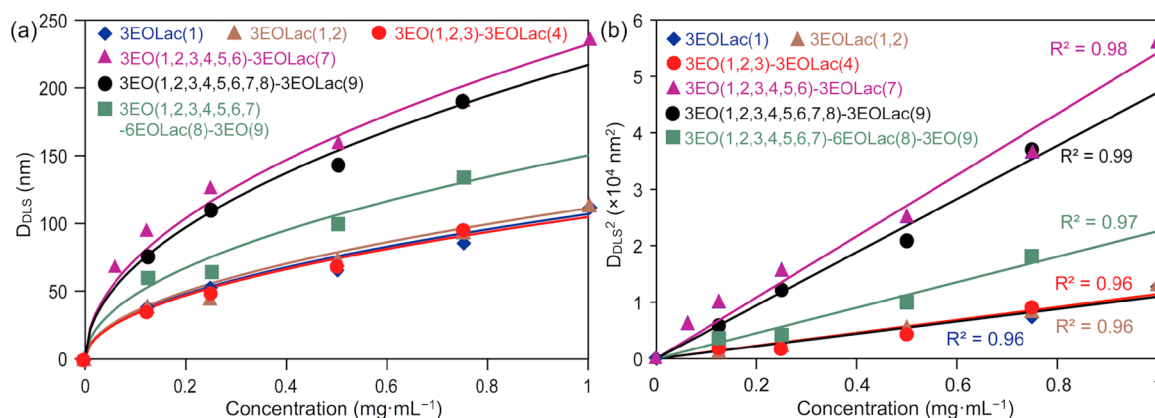


Figure 5. Concentration dependence of the (a) diameter (D_{DLS} , in nm) and (b) square of the diameter (D_{DLS}^2) of GDSs self-assembled by Lac-containing Janus-GDs in PBS. R^2 = coefficient of determination.

and this agrees with the increasing size of the vesicles following the order 2-Lac < 3-Lac < 4-Lac (Figure 4). On the other hand, the size of 4-Lac is almost identical with that of 5a-Lac and 5b-Lac, even though their molecular weights are not identical. More surprisingly, the GDSs formed by 6a-Lac and 6b-Lac shrink significantly. The complexity of the chemical structure of these Janus-GDs rendered the mechanism of self-assembly rather complex, and acquisition of a greater understanding of this self-

assembly process by computer simulations is currently in progress. In addition, it is important to notice that testing with DLS gave polydispersities (PDI) between 0.14 and 0.30. These values indicate monodisperse vesicles.

On the basis of the results previously reported by our laboratory, the sizes of “twin–twin”^{11b} or “single–single”^{11c} Janus dendrimerosomes were predictable by their concentration. The sizes (diameters) could be calculated from the thickness of

Table 1. Comparison of the Size of Various Lac-Containing Glycodendrimersomes Predicted by Diameter–Concentration Correlation and Size Determined by DLS at Lac = 0.1 mM in PBS

glycodendrimersomes	a ($D^2 = aC$) ^a	concn (mg·mL ⁻¹)	D_{pred} ^b (nm)	D_{DLS} (nm)	error ^c (%)
3EOLac(1)	11 426	0.109	35	39	9.1
3EOLac(1,2)	12 360	0.108	37	38	3.5
3EO(1,2,3)-3EOLac(4)	10 963	0.229	52	51	1.8
3EO(1,2,3,4,5,6)-3EOLac(7)	53 910	0.418	150	151	0.3
3EO(1,2,3,4,5,6,7,8)-3EOLac(9)	47 130	0.452	146	145	1.0
3EO(1,2,3,4,5,6,7)-6EOLac(8)-3EO(9)	22 565	0.466	103	100	2.5

^aEquations are derived from the linear correlation between the square of the diameter (D^2) and the mass concentration (C) in Figure 5, and a is the constant of the equation. ^bThe predicted diameter (D_{pred}) is calculated according to the equation $D^2 = aC$. ^cError is the absolute value calculated according to the equation $\text{error} = [(D_{\text{pred}} - D_{\text{DLS}})/D_{\text{pred}}] \times 100\%$.

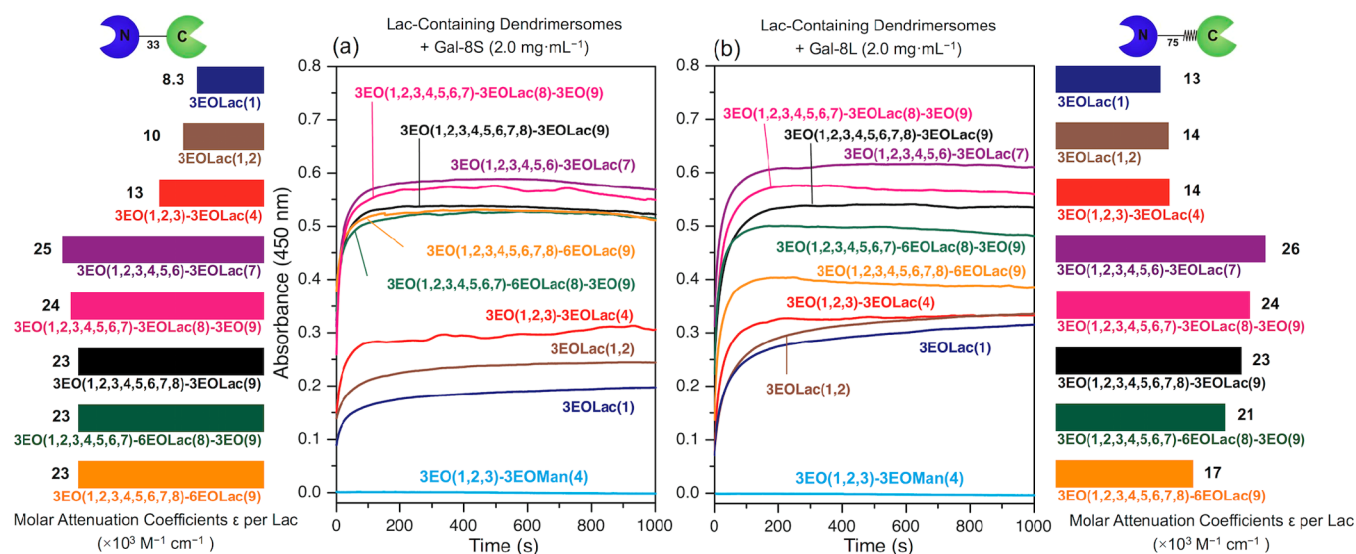


Figure 6. Agglutination assays between different Lac-containing GDSs at identical concentrations of Lac and two Gal-8 natural variants. Lac-containing GDSs (0.1 mM of Lac in 900 μL of PBS) were incubated with (a) Gal-8S or (b) Gal-8L (2 mg·mL⁻¹ in 100 μL of PBS). The molar attenuation coefficient, $\epsilon = A/(cl)$, was adapted from the Beer–Lambert law, where A = plateau OD value, c = molar concentration of Lac, and l = semimicrocuvette path length (0.23 cm). Control experiments were carried out by incubating 3-Man^{9b} [3EO(1,2,3)-3EOMan(4)] and 0.1 mM Man in 900 μL of PBS; its chemical structure is described in Scheme S8 (SI) with Gal-8S/8L (2 mg·mL⁻¹ in 100 μL of PBS).

the bilayer and the concentration of dendrimer solution. Furthermore, the square of the dendrimer diameter exhibits a linear correlation with the concentration. In the current study, all the Janus-GDs self-assembled into unilamellar vesicles with predictable dimension in PBS in a suitable range of concentration, as indicated in Figure 5. It should be noted that since the sizes of the isomeric pairs **5a**-/**5b**-Lac and **6a**-/**6b**-Lac were identical, **5b**-Lac [3EO(1,2,3,4,5,6,7,8)-3EOLac(9)] and **6a**-Lac [3EO(1,2,3,4,5,6,7)-6EOLac(8)-3EO(9)] were chosen as representative cases for the isomers. Figure 5a shows the experimental diameter values obtained from DLS experiments. When converting into the square of the diameter, as shown in Figure 5b, the mass concentration of each Janus-GD is proportional to the square of the diameter of the corresponding vesicle. This physically significant correlation was consistent with previous conclusions.^{11b,c} The curves in Figure 5a can therefore be used as a convenient calibration tool^{11b} to predict the size of the vesicles in the concentration range from 0 to 1 mg·mL⁻¹. The reliability of this prediction was validated by the results summarized in Table 1. The measured sizes of the GDSs agree with the predicted values at the final Lac concentration of 0.1 mM.

Supramolecular Models of Biological Membranes Containing Multivalent Glycan Ligands with Program-

mable Density, Sequence, and Topology of Presentation.

These GDSs provide a valuable toolbox to dissect the contribution of diverse parameters of spatial display on the bioactivity toward lectins. To add physiological relevance, a human lectin, the tandem-repeat-type galectin-8 (Gal-8), was examined. Gal-8 has recently been discovered to be a potent sensor for endosome/lysosome integrity¹² via its glycan binding and switching on of the autophagy machinery. It is also a matricellular modulator of adhesion and migration, with further effector capacity on cell growth.¹³ Its occurrence in two isoforms is caused by alternative splicing so that the two carbohydrate recognition domains (CRD) are connected by a peptide linker composed of 33 or 75 amino acids (Gal-8S/8L) (Figure SF2, SI). The functional relevance of the length of linker is so far unknown. The agglutination assays of all GDSs with Gal-8 were monitored by UV–vis spectroscopy for 1000 s so that the optical density (OD) value of all GDSs could reach a plateau (Figure 6). Before the study of the influence of spatial display of glycan ligands on the bioactivity of GDSs, nonselective binding was rigorously excluded by control experiments testing a suspension of GDSs with a noncognate sugar headgroup, i.e., D-mannose for Gal-8 (Figure 6), and with a nonspecific lectin, i.e., GDS from 3-Lac with ConA (Figure SF3, SI). Additional control experiments were reported in Figure SF26, SI of ref 9a, Figure SF5, SI of ref

9b, Figure SF2, SI of ref 9c, and Figures 4–6 of ref 9d. The absence of secondary interactions during the agglutination process were demonstrated by saturating Gal-8S with 100 mM D-lactose and perform the agglutination with GDSs from 3-Lac (Figure SF4, SI). No agglutination was observed in this experiment. However, the control experiment of Gal-8S containing 100 mM D-fructose provided the expected agglutination of GDSs from 3-Lac (Figure SF4, SI). Finally, the addition of 100 mM D-lactose 100 s after the agglutination of the GDSs from 3-Lac with Gal-8S provided quantitative dissociation and therefore demonstrated the absence of secondary interactions during the agglutination process (Figure SF5, SI).

In the first set of agglutination experiments, the molar concentration of Lac in all vesicles was maintained at 0.1 mM before incubation with Gal-8. In order to better quantify the relative agglutination activity of each type of Lac-containing vesicle, the molar attenuation coefficient per Lac (ϵ) was calculated according to the Beer–Lambert law ($A = \epsilon cl$), where A , c , and l respectively stand for the plateau value of OD, the molar concentration of Lac, and the path length of light that is equal to the width of the cuvette. This is valid under the assumption that there is no lysis of GDSs during the course of the agglutination assay. This assumption was validated previously by cryo-TEM^{9a,c} experiments that, in agreement with the mechanical properties of GDSs,^{9a,11a,b} supported their expected shape integrity during the agglutination process. The increase of OD value from Figure 6 is therefore the result of cross-linking of intact and undeformed GDSs. Therefore, the results of GDSs integrity during agglutination and the absence of secondary interactions is in agreement with isothermal titration calorimetry (ITC) and hemagglutination experiments reported for Gal-8.^{13c}

As an internal control, the series of 1-Lac, 2-Lac, and 3-Lac headgroup display was first tested with Gal-8S. Confirming previous experience,^{9d} a grading of activity was observed with the molar attenuation coefficient ϵ increasing from 8.3 for 1-Lac to 10 for 2-Lac and to $13 \times 10^3 \text{ M}^{-1}\cdot\text{cm}^{-1}$ for 3-Lac (Figure 6a). Indeed, the binding experiments in Figure 6 reveal a different range of responses for all GDSs, although their contact sites for Gal-8, i.e., the disaccharide Lac, are identical. This therefore underscores the influence of spatial factors. The already significant reactivity of 3-Lac was raised by up to 2-fold by altering the mode of presentation to 4-Lac, despite the reduced density of Lac. Of note, the compounds 4-Lac vs 5-Lac/6-Lac also likely differ in degree of lateral flexibility when self-assembling. This second factor concerns the possibility of a physiological elongation. It is realized either within the glycan chain, most prominently by adding *N*-acetylglucosamine repeats especially to the β 1,6-branch of complex-type *N*-glycans and the core 2/4 of mucin-type *O*-glycans, or within the scaffold by incorporation of long-chain fatty acids into the ceramide backbone of glycosphingolipids.¹⁴ Intuitively, such an extension should make the sugar headgroup especially accessible for lectin binding, as delineated for sulfatides with a C24-long anchor within apical transport processes in enterocyte-like cells by a human galectin.¹⁵ In contrast to the intuitive expectations, an extension of the linker (in 6a/b-Lac) did not lead to an increase of OD, since 5a/b-Lac with identical structure but shorter linker length were more conducive to yield aggregates (Figure 6). The comparison between 5a/b-Lac and 6a/b-Lac implies that an extended arm may allow backfolding to the surface of vesicles, which restricts headgroup accessibility or compromises stability of the trans-interaction of lectins. In summary, the highest signal was seen with 4-Lac as building block, and this indicates that

there could be an optimal sequence and density of glycan ligands to ensure the high level of their bioactivity.

We also tried to study the impact of length variation of the natural linker in Gal-8, if there is any. Instead of the rigid positioning of the four binding sites in concanavalin A (ConA),¹⁶ the linker between the two carbohydrate-binding domains of Gal-8 may furnish spatial adaptability, both rotationally and laterally. Whether the length extension of the natural linker of Gal-8 will affect its capacity for agglutination and sensitivity to surface design is answered in Figure 6. Fine-tuning by structural changes, for example between 6a-Lac and 6b-Lac, is in this case achievable, making Gal-8L more sensitive [$(21 \text{ vs } 17) \times 10^3 \text{ M}^{-1}\cdot\text{cm}^{-1}$ in Figure 6b] to changes in Lac display than Gal-8S [$(23 \text{ vs } 23) \times 10^3 \text{ M}^{-1}\cdot\text{cm}^{-1}$ in Figure 6a]. This difference nourishes the idea of higher spatial adaptability with longer linker length for this adhesion/growth-regulatory tissue effector.

It is instructive to compare the agglutination data from Figure 6 with the rate change in turbidity, k , of the same GDSs with Gal-8S (in blue) and Gal-8L (in red) from Figure 7. Since the

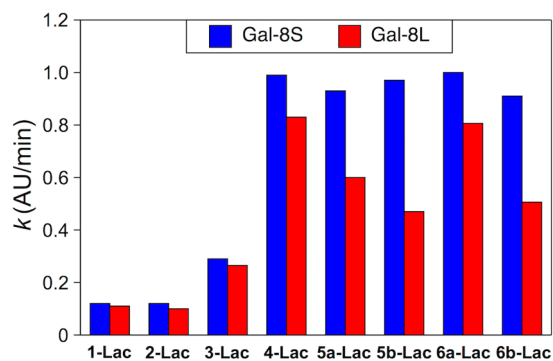


Figure 7. Rate of change in turbidity, k , of GDSs with Gal-8S (blue) and Gal-8L (red) calculated from the data in Figure 6 at $t_{0.5}$, where $t_{0.5}$ is the time at which the observed absorbance is equal to half of the plateau absorbance. Binding was too fast ($t_{0.5} \approx 5\text{--}20$ s) and the initial rate could not be determined. The initial rate is higher than the rate at $t_{0.5}$; hence, the calculated values of k presented here represent an underestimate of the true initial rate.

agglutination process is over in about 100 s, the initial rate was determined at $t_{0.5} \approx 5\text{--}20$ s in order to have a fair comparison of the rates from different processes; therefore, these values are underestimated. Nevertheless, they demonstrate the same trend as the data from Figure 6.

GDSs present the carbohydrates both on the interior and exterior surface of the supramolecular assemblies (Figure 4). It is not yet known at this time if any of the exterior surface carbohydrates may be or not quantitatively available for binding and to what extent they can be hidden within the GDS structure. Nevertheless, an indication that most of the carbohydrates from the outer surface of the GDSs are available for binding was provided by previous coassembly experiments performed with amphiphilic Janus glycodendrimers containing binding and nonbinding carbohydrates. These mixed binding–nonbinding GDSs demonstrated an increase in agglutination parallel with the increase in the concentration of the binding sugar.^{9d}

However, Figure 6 does not take into consideration that a constant concentration of Lac at 0.1 mM results in a range of diameters for the various GDSs. When the concentration of a specific Janus-GD is kept constant, it is expected that the bioactivity of the GDSs is size-dependent.^{9a} Thus, experiments to investigate the relationship between vesicle size and agglutina-

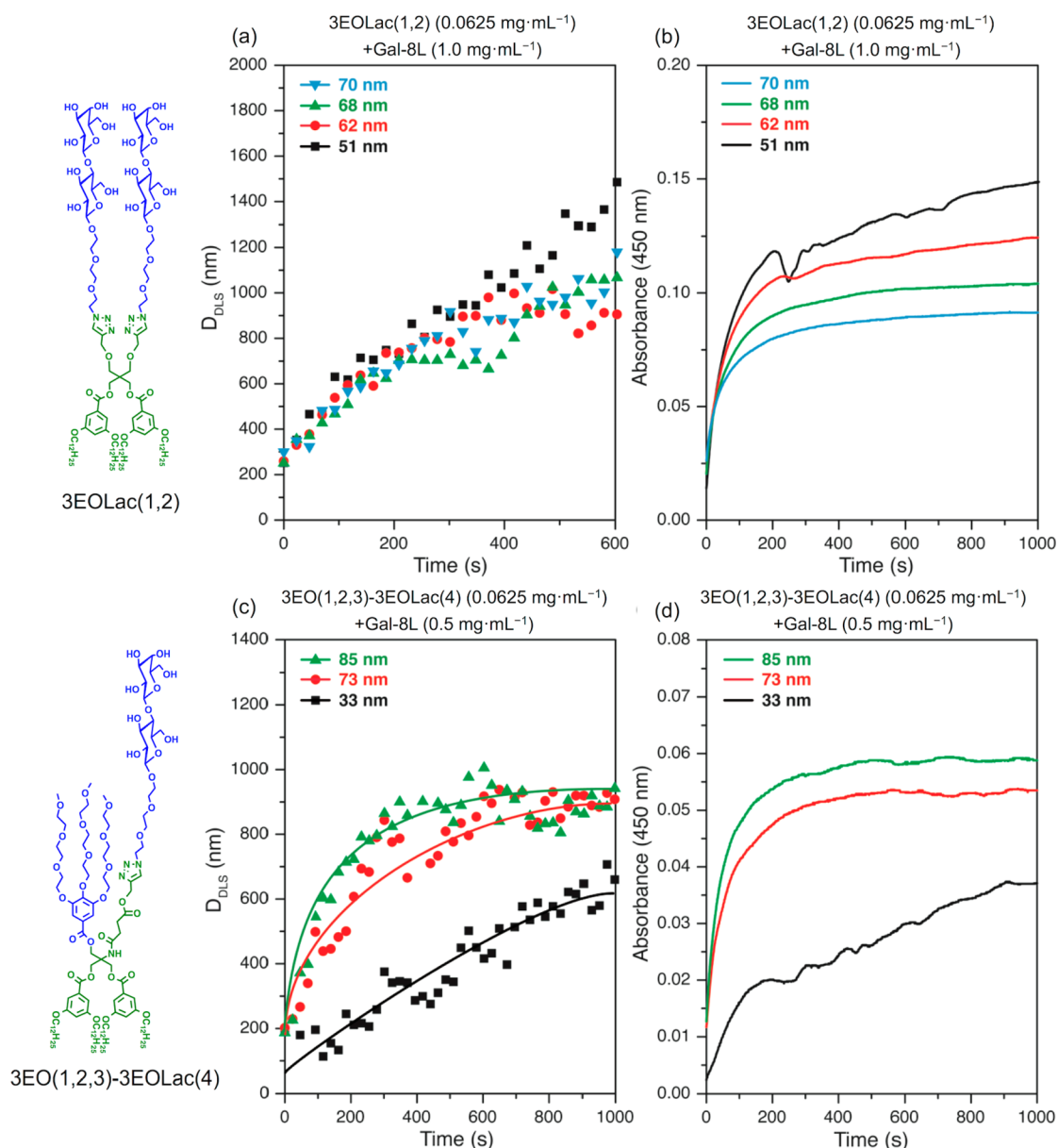


Figure 8. Agglutination of 2-Lac [3EOLac(1,2), 900 μ L, 0.0625 mg·mL⁻¹] and 3-Lac [3EO(1,2,3)-3EOLac(4) vesicles, 900 μ L, 0.0625 mg·mL⁻¹] GDSs of different sizes in the presence of Gal-8L (100 μ L, 0.5 or 1.0 mg·mL⁻¹) in PBS. The evolution of sizes of GDS–lectin aggregates was monitored by DLS (a and c) and UV–vis spectroscopy (b and d).

tion were performed. The impact of this parameter was considered with 2-Lac [3EOLac(1,2)] (Figure 8a,b) and 3-Lac [3EO(1,2,3)-3EOLac(4)] (Figure 8c,d) as two representative examples. These GDSs with identical concentration but different dimension were prepared by a successive dilution method (Figure SF1, SI). Immediately after Gal-8L was incubated with the GDSs, the evolution of size of GDS–lectin aggregates was monitored by DLS (Figure 8a,c) and UV–vis spectroscopy over a period of 600 s (Figure 8b,d). As determined by DLS, the fastest agglutination was provided by the smallest GDSs self-assembled by 2-Lac (Figure 8a). The plateau value of OD shows that the smallest size led to the highest bioactivity of the GDSs (Figure 8b). On the contrary, in the investigated range of dimensions, both the rate of binding and the bioactivity of the GDSs self-assembled by 3-Lac increased with increasing size (Figure 8c,d). The opposite tendency implies that the impact of size on bioactivity is specific rather than general for GDSs formed

by Janus-GDs having different structural frameworks, with possible ramifications for exosome/microvesicle recognition in situ. Thus, the conclusions made from Figure 6 had to be verified with additional experimentation that corrects for vesicle size.

By applying the prediction method illustrated in the previous section, all GDSs of identical size ($D_{DLS} = 63 \pm 3$ nm) were prepared from the corresponding Janus-GDs with different concentration. Their agglutination assays were again carried out with Gal-8. Inevitably, the concentration of all Janus-GDs cannot be kept constant in the case of identical size, but the impact of concentration can easily be excluded by calculation of the molar attenuation coefficient per Lac (ϵ) (Figure 9), yielding a set of data that controls for both size and concentration of the various GDSs. The ϵ value can evaluate their relative bioactivities due to the identical size with similar curvature and ratio of carbohydrates outside and inside the GDSs membranes. This series of binding experiments showed similar tendency in both

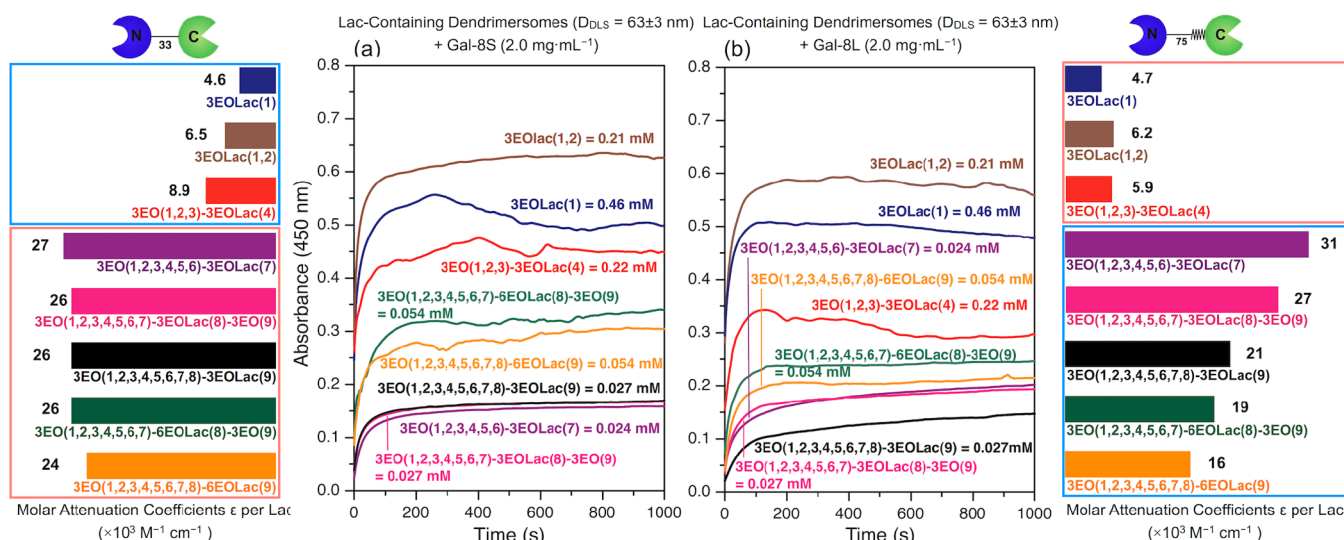


Figure 9. Agglutination assays between different GDSs of identical sizes. (a) Gal-8S ($2 \text{ mg}\cdot\text{mL}^{-1}$ in $100 \mu\text{L}$ of PBS) or (b) Gal-8L ($2 \text{ mg}\cdot\text{mL}^{-1}$ in $100 \mu\text{L}$ of PBS) was incubated with Lac-containing GDSs ($D_{DLS} = 63 \pm 3 \text{ nm}$, in $900 \mu\text{L}$ of PBS). The molar attenuation coefficient, $\epsilon = A/(cl)$, was adapted from Beer–Lambert law, where A = plateau OD value, c = molar concentration of Lac, and l = semimicrocuvette path length (0.23 cm). The boxes divide the GDSs into two groups: small Janus-GDs (top) and large Janus-GDs (bottom). The blue boxes indicate relatively high sensitivity and the red boxes indicate comparatively low sensitivity of lectins toward different glycan topologies.

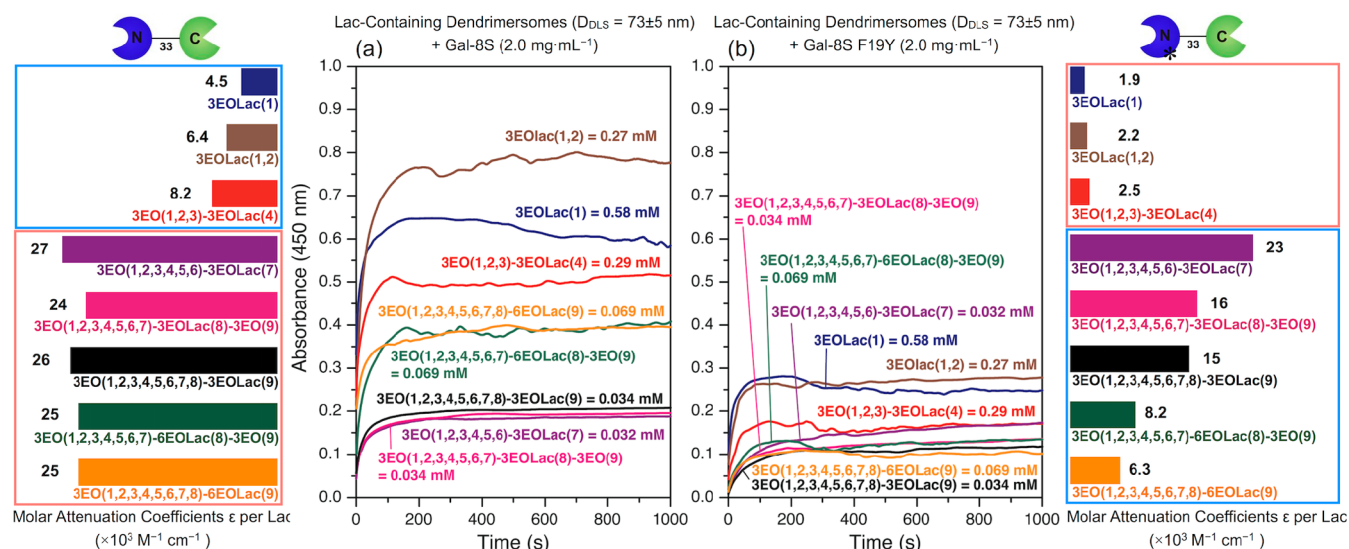


Figure 10. Agglutination assays between different GDSs of identical size. (a) Gal-8S ($2 \text{ mg}\cdot\text{mL}^{-1}$ in $100 \mu\text{L}$ of PBS) or (b) Gal-8S F19Y ($2 \text{ mg}\cdot\text{mL}^{-1}$ in $100 \mu\text{L}$ of PBS) was incubated with Lac-containing GDSs ($D_{DLS} = 73 \pm 5 \text{ nm}$, in $900 \mu\text{L}$ of PBS). The molar attenuation coefficient, $\epsilon = A/(cl)$, was adapted from Beer–Lambert law, where A = plateau OD value, c = molar concentration of Lac, and l = semimicrocuvette path length (0.23 cm). The boxes divide the GDSs into two groups: small Janus-GDs (top) and large Janus-GDs (bottom). The blue boxes indicate high sensitivity and the red boxes indicate low sensitivity of lectins toward different glycan topologies.

cases of Gal-8S and Gal-8L, as presented in Figure 6, and this further confirms that the spatial display of glycan ligands significantly affects the relative bioactivity of the GDSs.

As reported previously in our laboratory, a single-site mutation of the peptide linker of wild-type (WT) Gal-8S can impair significantly its cross-linking activity with GDSs self-assembled by 3-Lac.^{9d} Extending from 3-Lac to all Janus-GDs with different structural pattern in the current study, we compared the bioactivity of WT Gal-8S with that of Gal-8S F19Y (the mutated form) (Figure SF2, SI) for all Lac-containing GDSs of identical size ($D_{DLS} = 73 \pm 5 \text{ nm}$) (Figure 10). In line with previous results,^{9d} a significant drop in agglutination level from WT Gal-8S to the F19Y mutant was observed for all GDSs. Of note,

different GDSs showed different sensitivity toward the impaired function of Gal-8. For example, 30%, 85%, and 25% of the original bioactivity was retained for 3-Lac, 4-Lac, and 6b-Lac when they were incubated with F19Y, respectively. As can be judged from the value of the molar attenuation coefficient (ϵ), Gal-8S always exhibited the highest affinity with 4-Lac, regardless of its WT or mutated form (Figure 10).

After excluding both the factors of dimension of GDSs and concentration of Lac, the coverage of Lac on GDS surfaces decreased from 100% for 1-Lac and 2-Lac to 25% for 3-Lac (containing a 3/1 ratio of 3EO/Lac), 14% for 4-Lac (containing a 6/1 ratio of 3EO/Lac), and 11% for 5a-, 5b-, 6a-, and 6b-Lac (all containing a 8/1 ratio of 3EO/Lac). For the series 1-, 2-, 3-

and 4-Lac, the tendency of relative bioactivity toward Gal-8 variants always increased significantly, reaching a maximum ϵ value for 4-Lac (6/1 of 3EO/Lac). Compared to 4-Lac, the series 5a-, 5b-, 6a-, and 6b-Lac demonstrated a decrease in relative bioactivity, but they showed greater values than 1-, 2-, and 3-Lac. It is possible that the decreased Lac coverage on 4-Lac compared to 1-, 2-, and 3-Lac could provide better accessibility, resulting in the most efficient protein–sugar interactions. However, further Lac dilution, as in the cases of 5a-, 5b-, 6a-, and 6b-Lac, may reduce the necessary quantity of ligand epitopes for binding, offsetting any added steric benefit of greater dilution. Thus, 4-Lac provides an optimal balance between Lac density and accessibility; even with a dilution factor of 1/7, an increased relative bioactivity factor of 6 (Gal-8S), 7 (Gal-8L), or 12 (Gal-8S F19Y) was still seen, compared with 1-Lac.

It is also worth noting that, regarding the behavior of binding of all GDSs, they can be categorized into two groups: the group of small Janus-GDs, including 1-, 2-, and 3-Lac, and the group of large Janus-GDs, including 4-, 5a-, 5b-, 6a-, and 6b-Lac. The relative bioactivity of Gal-8S is clearly distinguishable for the group of small Janus-GDs, with their ϵ values being 4.8, 6.5, $8.9 \times 10^3 \text{ M}^{-1}\cdot\text{cm}^{-1}$ for 1-, 2-, and 3-Lac (blue box in Figure 9a), respectively, while the GDSs in the group of large Janus-GDs showed similar affinity toward the same lectin with $\epsilon = (24\text{--}27) \times 10^3 \text{ M}^{-1}\cdot\text{cm}^{-1}$ (red box in Figure 9a). On the other hand, this tendency is the opposite in the case of Gal-8L (Figure 9b) and Gal-8S F19Y (Figure 10b). Taking Gal-8L, for instance, the relative bioactivity of small Janus-GDs 1-, 2-, and 3-Lac was fairly similar to $\epsilon = (4.7\text{--}6.2) \times 10^3 \text{ M}^{-1}\cdot\text{cm}^{-1}$ (red box in Figure 9b), whereas the large Janus-GDs showed significantly different relative activities with $\epsilon = 31, 27, 21, 19,$ and $16 \times 10^3 \text{ M}^{-1}\cdot\text{cm}^{-1}$ for 4-, 5a-, 5b-, 6a-, and 6b-Lac (blue box in Figure 9b). This discrimination ability toward different lectins could be amplified by “GDS array patterning” and used as the principle for their sensing and identification.

CONCLUSIONS

The current study employed a rational chemical design strategy involving sequence- and density-defined parameters to create a library of amphiphilic Janus-GDs that self-assemble into GDSs with programmable glycan topology on their surface. These GDSs can evidently be designed to mimic the spatial properties of biological membranes; therefore, they provide a versatile tool for research in glycobiology. Agglutination assays with the human lectin Gal-8 unraveled the impact of density, sequence, and topology of the glycans on the bioactivity of the GDS. Various modes of sugar presentation on the GDS surface led to conspicuously different extents of stable trans-interactions that can be used to study structure–activity correlations with relevance for understanding how glycan display on biological membranes and lectin design team up for their intriguing functions. Since the influence of ligand structure on binding processes of biological membranes is incompletely understood^{5d,k} and contradictory results were reported with different models,^{5d,k,7a} the up to 12 times increased relative agglutination activity at 7 times lower Lac concentration observed for 4-Lac with Gal-8S F19Y was unpredictable and is a remarkable conclusion of these investigations. Thus, this supramolecular platform offers not only the highest activity but also sensor capability and versatility for establishing and exploiting structure–activity relationships of far-reaching biomedical relevance. The detailed presentation of Lac on the surface of these GDSs requires additional experiments. Nevertheless, we

believe that these results will impact the design of more efficient glycopolymers, glycopeptides, glycodendrimers, and of any other multivalent glycoconjugates by decreasing the density of the carbohydrate while a proper and well-defined-sequence is employed. Last but not least, our laboratory’s approach to discovery and prediction by screening rationally designed libraries of building blocks¹⁷ has been shown to be extremely efficient when applied to amphiphilic Janus dendrimers, their dendrimersomes,¹² amphiphilic Janus-GDs, and their GDSs.⁹ These investigations provided substantial progress in the field of synthetic vesicles and liposomes.¹⁸ The generality of the sequence- and density-defined presentation of ligands on the concept of multivalency⁸ reported here is currently being expanded to additional GDSs libraries with more complex structure, different glycan ligands, as well as to other classes of ligands.

ASSOCIATED CONTENT

Supporting Information

The Supporting Information is available free of charge on the ACS Publications website at DOI: 10.1021/jacs.5b08844.

Synthetic procedures with complete structural and self-assembly analysis, sample preparation, and experimental protocol (PDF)

AUTHOR INFORMATION

Corresponding Author

*percec@sas.upenn.edu

Notes

The authors declare no competing financial interest.

ACKNOWLEDGMENTS

Financial support from the National Science Foundation (grants DMR-1066116 and DMR-1120901), the P. Roy Vagelos Chair at the University of Pennsylvania, and the Humboldt Foundation (all to VP), the National Science Foundation (grant DMR-1120901 to MLK) and the EC Seventh Framework Programme (GLYCOPHARM) is gratefully acknowledged. The authors also thank Dr. H.-J. Sun for performing one cryo-TEM experiment.

REFERENCES

- (1) (a) Thaler, C. D.; Cardullo, R. A. *J. Biol. Chem.* **1996**, *271*, 23289–23297. (b) Clark, G. F.; Dell, A. *J. Biol. Chem.* **2006**, *281*, 13853–13856.
- (2) (a) Fevrier, B.; Raposo, G. *Curr. Opin. Cell Biol.* **2004**, *16*, 415–421. (b) Valadi, H.; Ekström, K.; Bossios, A.; Sjöstrand, M.; Lee, J. J.; Lötvall, J. O. *Nat. Cell Biol.* **2007**, *9*, 654–659. (c) EL Andaloussi, S.; Mäger, I.; Breakefield, X. O.; Wood, M. J. A. *Nat. Rev. Drug Discovery* **2013**, *12*, 347–357. (d) Raposo, G.; Stoorvogel, W. *J. Cell Biol.* **2013**, *200*, 373–383.
- (3) (a) Sharon, N.; Lis, H. *Science* **1972**, *177*, 949–959. (b) Lee, Y. C.; Lee, R. T. *Acc. Chem. Res.* **1995**, *28*, 321–327. (c) Lis, H.; Sharon, N. *Chem. Rev.* **1998**, *98*, 637–674. (d) Gabius, H.-J.; André, S.; Jiménez-Barbero, J.; Romero, A.; Solis, D. *Trends Biochem. Sci.* **2011**, *36*, 298–313. (e) Lepenies, B.; Lee, J.; Sonkaria, S. *Adv. Drug Delivery Rev.* **2013**, *65*, 1271–1281. (f) André, S.; Kaltner, H.; Manning, J. C.; Murphy, P. V.; Gabius, H.-J. *Molecules* **2015**, *20*, 1788–1823.
- (4) (a) Aoi, K.; Tsutsumiuchi, K.; Okada, M. *Macromolecules* **1994**, *27*, 875–877. (b) Allen, J. R.; Harris, C. R.; Danishefsky, S. J. *J. Am. Chem. Soc.* **2001**, *123*, 1890–1897. (c) Kramer, J. R.; Deming, T. J. *J. Am. Chem. Soc.* **2010**, *132*, 15068–15071. (d) Kramer, J. R.; Deming, T. J. *Polym. Chem.* **2014**, *5*, 671–682. (e) Krannig, K.-S.; Sun, J.; Schlaad, H. *Biomacromolecules* **2014**, *15*, 978–984.
- (5) (a) Yamada, K.; Yamaoka, K.; Minoda, M.; Miyamoto, T. *J. Polym. Sci., Part A: Polym. Chem.* **1997**, *35*, 255–261. (b) Horan, N.; Yan, L.;

- Isobe, H.; Whitesides, G. M.; Kahne, D. *Proc. Natl. Acad. Sci. U. S. A.* **1999**, *96*, 11782–11786. (c) Matsuura, K.; Hibino, M.; Yamada, Y.; Kobayashi, K. *J. Am. Chem. Soc.* **2001**, *123*, 357–358. (d) Cairo, C. W.; Gestwicki, J. E.; Kanai, M.; Kiessling, L. L. *J. Am. Chem. Soc.* **2002**, *124*, 1615–1619. (e) Polizzotti, B. D.; Küick, K. L. *Biomacromolecules* **2006**, *7*, 483–490. (f) Geng, J.; Mantovani, G.; Tao, L.; Nicolas, J.; Chen, G.; Wallis, R.; Mitchell, D. A.; Johnson, B. R. G.; Evans, S. D.; Haddleton, D. M. *J. Am. Chem. Soc.* **2007**, *129*, 15156–15163. (g) Godula, K.; Bertozzi, C. R. *J. Am. Chem. Soc.* **2010**, *132*, 9963–9965. (h) Ruff, Y.; Buhler, E.; Candau, S.-J.; Kesselman, E.; Talmon, Y.; Lehn, J.-M. *J. Am. Chem. Soc.* **2010**, *132*, 2573–2584. (i) Ponader, D.; Wojcik, F.; Beceren-Braun, F.; Dervede, J.; Hartmann, L. *Biomacromolecules* **2012**, *13*, 1845–1852. (j) Miura, Y. *Polym. J.* **2012**, *44*, 679–689. (k) Kiessling, L. L.; Grim, J. C. *Chem. Soc. Rev.* **2013**, *42*, 4476–4491. (l) Zhang, Q.; Haddleton, D. M. *Adv. Polym. Sci.* **2013**, *262*, 39–60. (m) Jimenez Blanco, J. L.; Ortiz Mellet, C.; Garcia Fernandez, J. M. *Chem. Soc. Rev.* **2013**, *42*, 4518–4531. (n) Ponader, D.; Maffre, P.; Aretz, J.; Pussak, D.; Ninnemann, N. M.; Schmidt, S.; Seeberger, P. H.; Rademacher, C.; Nienhaus, G. U.; Hartmann, L. *J. Am. Chem. Soc.* **2014**, *136*, 2008–2016.
- (6) (a) Roy, R.; Zanini, D.; Meunier, S. J.; Romanowska, A. *J. Chem. Soc., Chem. Commun.* **1993**, 1869–1993. (b) Turnbull, W. B.; Kalovidouris, S. A.; Stoddart, J. F. *Chem. - Eur. J.* **2002**, *8*, 2988–3000. (c) Woller, E. K.; Walter, E. D.; Morgan, J. R.; Singel, D. J.; Cloninger, M. J. *J. Am. Chem. Soc.* **2003**, *125*, 8820–8826. (d) Wang, S.-K.; Liang, P.-H.; Astronomo, R. D.; Hsu, T.-L.; Hsieh, S.-L.; Burton, D. R.; Wong, C.-H. *Proc. Natl. Acad. Sci. U. S. A.* **2008**, *105*, 3690–3695. (e) Thomas, B.; Berthet, N.; Garcia, J.; Dumy, P.; Renaudet, O. *Chem. Commun.* **2013**, *49*, 10796–10798. (f) Munoz, E. M.; Correa, J.; Riguera, R.; Fernandez-Megia, E. *J. Am. Chem. Soc.* **2013**, *135*, 5966–5969. (g) Chabre, Y. M.; Roy, R. *Chem. Soc. Rev.* **2013**, *42*, 4657–4708. (h) Appelhans, D.; Klajnert-Maculewicz, B.; Janaszewska, A.; Lazniewska, J.; Voit, B. *Chem. Soc. Rev.* **2015**, *44*, 3968–3996. (i) Roy, R.; Shiao, T. C. *Chem. Soc. Rev.* **2015**, *44*, 3924–3941.
- (7) (a) Grant, C. W. M.; Peters, M. W. *Biochim. Biophys. Acta, Rev. Biomembr.* **1984**, *779*, 403–422. (b) DeFrees, S. A.; Phillips, L.; Guo, L.; Zalipsky, S. *J. Am. Chem. Soc.* **1996**, *118*, 6101–6104. (c) Voskuhl, J.; Stuart, M. C. A.; Ravoo, B. J. *Chem. - Eur. J.* **2010**, *16*, 2790–2796. (d) Kramer, J. R.; Rodriguez, A. R.; Choe, U.-J.; Kamei, D. T.; Deming, T. J. *Soft Matter* **2013**, *9*, 3389–3395. (e) Jayaraman, N.; Maiti, K.; Naresh, K. *Chem. Soc. Rev.* **2013**, *42*, 4640–4656. (f) Chmielewski, M. J.; Buhler, E.; Candau, J.; Lehn, J.-M. *Chem. - Eur. J.* **2014**, *20*, 6960–6977.
- (8) (a) Mammen, M.; Choi, S.-K.; Whitesides, G. M. *Angew. Chem., Int. Ed.* **1998**, *37*, 2754–2794. (b) Lundquist, J. J.; Toone, E. J. *Chem. Rev.* **2002**, *102*, 555–578. (c) Fasting, C.; Schalley, C. A.; Weber, M.; Seitz, O.; Hecht, S.; Kokschi, B.; Dervede, J.; Graf, C.; Knapp, E.-W.; Haag, R. *Angew. Chem., Int. Ed.* **2012**, *51*, 10472–10498.
- (9) (a) Percec, V.; Leowanawat, P.; Sun, H.-J.; Kulikov, O.; Nusbaum, C. D.; Tran, T. M.; Bertin, A.; Wilson, D. A.; Peterca, M.; Zhang, S.; Kamat, N. P.; Vargo, K.; Moock, D.; Johnston, E. D.; Hammer, D. A.; Pochan, D. J.; Chen, Y.; Chabre, Y. M.; Shiao, T. C.; Bergeron-Brelek, M.; André, S.; Roy, R.; Gabius, H.-J.; Heiney, P. A. *J. Am. Chem. Soc.* **2013**, *135*, 9055–9077. (b) Zhang, S.; Moussodia, R.-O.; Sun, H.-J.; Leowanawat, P.; Muncan, A.; Nusbaum, C. D.; Chelling, K. M.; Heiney, P. A.; Klein, M. L.; André, S.; Roy, R.; Gabius, H.-J.; Percec, V. *Angew. Chem., Int. Ed.* **2014**, *53*, 10899–10903. (c) Zhang, S.; Moussodia, R.-O.; Murzeau, C.; Sun, H.-J.; Klein, M. L.; Vértésy, S.; André, S.; Roy, R.; Gabius, H.-J.; Percec, V. *Angew. Chem., Int. Ed.* **2015**, *54*, 4036–4040. (d) Zhang, S.; Moussodia, R.-O.; Vértésy, S.; André, S.; Klein, M. L.; Gabius, H.-J.; Percec, V. *Proc. Natl. Acad. Sci. U. S. A.* **2015**, *112*, 5585–5590.
- (10) (a) Kolb, H. C.; Finn, M. G.; Sharpless, K. B. *Angew. Chem., Int. Ed.* **2001**, *40*, 2004–2021. (b) Rostovtsev, V. V.; Green, L. G.; Fokin, V. V.; Sharpless, K. B. *Angew. Chem., Int. Ed.* **2002**, *41*, 2596–2599.
- (11) (a) Percec, V.; Wilson, D. A.; Leowanawat, P.; Wilson, C. J.; Hughes, A. D.; Kaucher, M. S.; Hammer, D. A.; Levine, D. H.; Kim, A. J.; Bates, F. S.; Davis, K. P.; Lodge, T. P.; Klein, M. L.; DeVane, R. H.; Aqad, E.; Rosen, B. M.; Argintaru, A. O.; Sienkowska, M. J.; Rissanen, K.; Nummelin, S.; Ropponen, J. *Science* **2010**, *328*, 1009–1014. (b) Peterca, M.; Percec, V.; Leowanawat, P.; Bertin, A. *J. Am. Chem. Soc.* **2011**, *133*, 20507–20520. (c) Zhang, S.; Sun, H.-J.; Hughes, A. D.; Draghici, B.; Lejniaks, J.; Leowanawat, P.; Bertin, A.; Otero De Leon, L.; Kulikov, O. V.; Chen, Y.; Pochan, D. J.; Heiney, P. A.; Percec, V. *ACS Nano* **2014**, *8*, 1554–1565. (d) Zhang, S.; Sun, H.-J.; Hughes, A. D.; Moussodia, R.-O.; Bertin, A.; Chen, Y.; Pochan, D. J.; Heiney, P. A.; Klein, M. L.; Percec, V. *Proc. Natl. Acad. Sci. U. S. A.* **2014**, *111*, 9058–9063.
- (12) (a) Thurston, T. L. M.; Wandel, M. P.; von Muhlinen, N.; Foeglein, A.; Randow, F. *Nature* **2012**, *482*, 414–418. (b) Meunier, E.; Dick, M. S.; Dreier, R. F.; Schürmann, N.; Broz, D. K.; Warming, S.; Roose-Girma, M.; Bumann, D.; Kayagaki, N.; Takeda, K.; Yamamoto, M.; Broz, P. *Nature* **2014**, *509*, 366–370.
- (13) (a) Zick, Y.; Eisenstein, M.; Goren, R. A.; Hadari, Y. R.; Levy, Y.; Ronen, D. *Glycoconjugate J.* **2002**, *19*, 517–526. (b) Eshkar Sebban, L.; Ronen, D.; Levartovsky, D.; Elkayam, O.; Caspi, D.; Aamar, S.; Amital, H.; Rubinow, A.; Golan, I.; Naor, D.; Zick, Y.; Golan, I. *J. Immunol.* **2007**, *179*, 1225–1235. (c) Ruiz, F. M.; Scholz, B. A.; Buzamet, E.; Kopitz, J.; André, S.; Menéndez, M.; Romero, A.; Solís, D.; Gabius, H.-J. *FEBS J.* **2014**, *281*, 1446–1464.
- (14) (a) Sandhoff, R. *FEBS Lett.* **2010**, *584*, 1907–1913. (b) Togayachi, A.; Narimatsu, H. *Trends Glycosci. Glycotechnol.* **2012**, *24*, 95–111.
- (15) Delacour, D.; Gouyer, V.; Zanetta, J.-P.; Drobecq, H.; Leteurtre, E.; Grard, G.; Moreau-Hannedouche, O.; Maes, E.; Pons, A.; André, S.; Le Bivic, A.; Gabius, H. J.; Manninen, A.; Simons, K.; Huet, G. *J. Cell Biol.* **2005**, *169*, 491–501.
- (16) Goldstein, I. J.; Poretz, R. D. In *The Lectins Properties, Functions and Applications in Biology and Medicine*; Goldstein, I. J., Liener, I. E., Sharon, N., Eds.; Academic: San Diego, CA, 1986; pp 233–247.
- (17) (a) Percec, V.; Cho, W.-D.; Ungar, G.; Yeardley, D. J. P. *J. Am. Chem. Soc.* **2001**, *123*, 1302–1315. (b) Percec, V.; Mitchell, C. M.; Cho, W.-D.; Uchida, S.; Glodde, M.; Ungar, G.; Zeng, X.; Liu, Y.; Balagurusamy, V. S. K.; Heiney, P. A. *J. Am. Chem. Soc.* **2004**, *126*, 6078–6094. (c) Percec, V.; Holerca, M. N.; Nummelin, S.; Morrison, J. J.; Glodde, M.; Smidrakal, J.; Peterca, M.; Rosen, B. M.; Uchida, S.; Balagurusamy, V. S. K.; Sienkowska, M. J.; Heiney, P. A. *Chem. - Eur. J.* **2006**, *12*, 6216–6241. (d) Percec, V.; Peterca, M.; Sienkowska, M. J.; Ilies, M. A.; Aqad, E.; Smidrakal, J.; Heiney, P. A. *J. Am. Chem. Soc.* **2006**, *128*, 3324–3334. (e) Percec, V.; Won, B. C.; Peterca, M.; Heiney, P. A. *J. Am. Chem. Soc.* **2007**, *129*, 11265–11278. (f) Rosen, B. M.; Wilson, D. A.; Wilson, C. J.; Peterca, M.; Won, B. C.; Huang, C.; Lipski, L. R.; Zeng, X.; Ungar, G.; Heiney, P. A.; Percec, V. *J. Am. Chem. Soc.* **2009**, *131*, 17500–17521.
- (18) (a) Ringsdorf, H.; Schlarb, B.; Venzmer, J. *Angew. Chem., Int. Ed. Engl.* **1988**, *27*, 113–158. (b) Kunitake, T. *Angew. Chem., Int. Ed. Engl.* **1992**, *31*, 709–726. (c) Thomas, J. L.; Tirrell, D. A. *Acc. Chem. Res.* **1992**, *25*, 336–342. (d) Guo, X.; Szoka, F. C. *Acc. Chem. Res.* **2003**, *36*, 335–341. (e) Torchilin, V. P. *Nat. Rev. Drug Discovery* **2014**, *13*, 813–827. (f) Allen, T. M.; Cullis, P. R. *Science* **2004**, *303*, 1818–1822.